RESEARCH ARTICLE

Key Points:
- Evapotranspiration (ET) dynamics were compared at two water-limited shrublands
- Precipitation seasonality influenced relationships between ET and forcing variables
- Soil moisture is the main control of ET when radiation and temperature are not limiting

Contrasting precipitation seasonality influences evapotranspiration dynamics in water-limited shrublands

Samuel Villarreal[1,2], Rodrigo Vargas[1], Enrico A. Yepez[3], Jose S. Acosta[2], Angel Castro[2,4], Martin Escoto-Rodriguez[2], Eulogio Lopez[2], Juan Martínez-Osuna[2], Julio C. Rodriguez[5], Stephen V. Smith[6], Enrique R. Vivoni[7], and Christopher J. Watts[8]

[1]Department of Plant and Soil Sciences, University of Delaware, Newark, Delaware, USA, [2]Department of Conservation Biology, Centro de Investigación Científica y de Educación Superior de Ensenada, Ensenada, Mexico, [3]Department of Water and Environmental Sciences, Instituto Tecnológico de Sonora, Ciudad Obregon, Mexico, [4]Observatorio Astronómico Nacional, Universidad Nacional Autónoma de Mexico, Ensenada, Mexico, [5]Department of Agriculture and Animal Husbandry, Universidad de Sonora, Hermosillo, Mexico, [6]Emeritus Professor of Oceanography, Department of Oceanography, University of Hawai'i at Mānoa, Honolulu, Hawaii, USA, [7]School of Earth and Space Exploration and School of Sustainable Engineering and the Built Environment, Arizona State University, Tempe, Arizona, USA, [8]Department of Physics, Universidad de Sonora, Hermosillo, Mexico

Abstract Water-limited ecosystems occupy nearly 30% of the Earth, but arguably, the controls on their ecosystem processes remain largely uncertain. We analyzed six site years of eddy covariance measurements of evapotranspiration (ET) from 2008 to 2010 at two water-limited shrublands: one dominated by winter precipitation (WP site) and another dominated by summer precipitation (SP site), but with similar solar radiation patterns in the Northern Hemisphere. We determined how physical forcing factors (i.e., net radiation (R_n), soil water content (SWC), air temperature (T_a), and vapor pressure deficit (VPD)) influence annual and seasonal variability of ET. Mean annual ET at SP site was $455 \pm 91 \, \text{mm yr}^{-1}$, was mainly influenced by SWC during the dry season, by R_n during the wet season, and was highly sensitive to changes in annual precipitation (P). Mean annual ET at WP site was $363 \pm 52 \, \text{mm yr}^{-1}$, had less interannual variability, but multiple variables (i.e., SWC, T_a, VPD, and R_n) were needed to explain ET among years and seasons. Wavelet coherence analysis showed that ET at SP site has a consistent temporal coherency with T_a and P, but this was not the case for ET at WP site. Our results support the paradigm that SWC is the main control of ET in water-limited ecosystems when radiation and temperature are not the limiting factors. In contrast, when P and SWC are decoupled from available energy (i.e., radiation and temperature), then ET is controlled by an interaction of multiple variables. Our results bring attention to the need for better understanding how climate and soil dynamics influence ET across these globally distributed ecosystems.

1. Introduction

Water-limited ecosystems cover over 30% of the global land surface area [*Schlesinger et al.*, 1990; *Loveland et al.*, 2000] and play a fundamental role in global biogeochemical cycles [*Rotenberg and Yakir*, 2010; *Poulter et al.*, 2014]. These ecosystems are characterized by having a nearly constant high evaporative demand due to high potential evapotranspiration (ETp) [*Lauenroth and Bradford*, 2009; *Sala and Lauenroth*, 2014] and large ranges in annual cumulative precipitation [*Noy-Meir*, 1973; *Lauenroth and Bradford*, 2009]. These conditions make biogeochemical processes in water-limited ecosystems highly sensitive to changes in the frequency and intensity of rainfall [*Austin et al.*, 2004; *Lauenroth and Bradford*, 2009; *Vargas et al.*, 2013a]. Despite the global extent of these ecosystems, research on how ecosystem processes respond to changing weather conditions still lags behind research performed in other ecosystems (e.g., temperate forests [*Baldocchi et al.*, 2012]). Furthermore, not all water-limited ecosystems are the same, because vegetation structure (e.g., grassland versus shrublands) or precipitation patterns (e.g., areas dominated by summer or winter precipitation) can vary substantially. Thus, there is a need to better understand these ecosystems to constrain global carbon and water balances [*Beer et al.*, 2010; *Jung et al.*, 2010] and improve the simulation of ecosystem fluxes by process-based models [*Méndez-Barroso et al.*, 2009; *Dietze et al.*, 2011; *Vivoni*, 2012; *Vargas et al.*, 2013a] that will provide information to predict impacts of global environmental change [*Maestre et al.*, 2012].
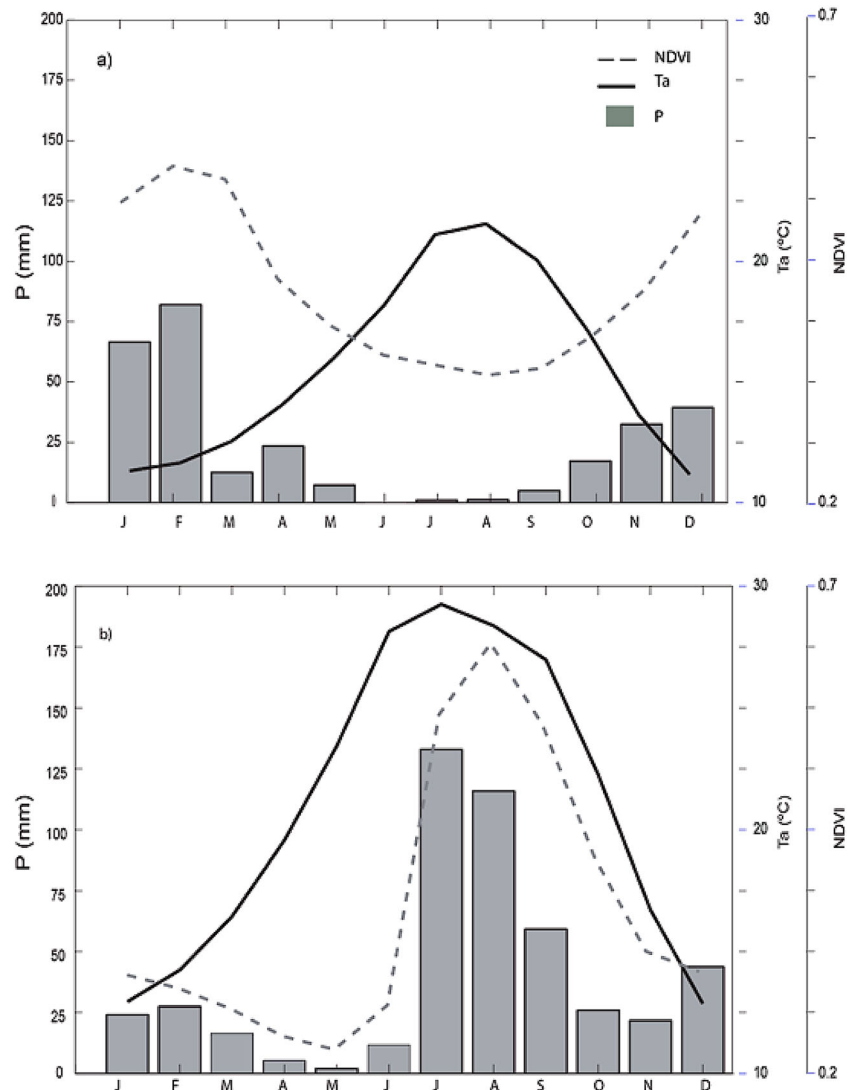
Figure 1. Mean monthly precipitation and temperature between 1980 and 2008, and mean monthly normalized difference vegetation index between 2008 and 2010, at the (a) winter precipitation (WP) and (b) summer precipitation (SP) sites.

In water-limited ecosystems, it is expected that differences in seasonal and annual ET dynamics will be largely influenced by precipitation variability [*Kurc and Small*, 2004; *Ryu et al.*, 2008; *Méndez-Barroso et al.*, 2014]. This is because ETp is relatively high for almost the entire year, and hence, precipitation patterns have a large influence on ET dynamics [*Potts et al.*, 2003; *Kurc and Small*, 2004] and other ecosystem processes such as primary productivity and soil CO_2 efflux [*Vargas et al.*, 2012b]. In light that precipitation patterns are not equal among all water-limited ecosystems (e.g., dominated by summer or winter precipitation), it is expected that dynamics between ET and water availability or ET and available energy vary among them [*Wang and Dickinson*, 2012]. These differences provide an excellent opportunity to test how ET responds to contrasting precipitation patterns along with similar radiation-temperature regimes (maximum during summer and minimum at winter) in water-limited ecosystems across sites dominated by summer or winter precipitation [*Scott et al.*, 2012].

Water-limited sites dominated by winter precipitation (WP) are, in general, characterized by dispersed rainfall events during the autumn-winter season (i.e., cool-season rainfall), when available energy (i.e., radiation and temperature) is relatively low compared to its maximum during summer [*Rana and Katerji*, 2000; *Ryu et al.*, 2008]. These WP sites are characteristic of Mediterranean climates where there is a decoupling between precipitation and available energy (Figure 1a), like the xeric Mediterranean climate shrubland associations of

California and Baja California [*Westman*, 1983]. In contrast, the sites dominated by summer precipitation (SP) are, in general, characterized by an intense rainfall season during the warm months (i.e., warm-season rainfall), when the available energy (i.e., radiation and temperature) reaches its annual maximum [*Perez-Ruiz et al.*, 2010]. These SP sites dominate the dry domain of the North American monsoon (NAM) including the Chihuahuan and Sonoran Deserts [*Weiss et al.*, 2004] where there is a coupling between precipitation (generated by local convection) and available energy (Figure 1b). These contrasting patterns influence different phenology responses, where the vegetation has a weak response to precipitation when it is decoupled from T_a (WP site; Figure 1a), and a stronger response to precipitation when it is in phase with T_a (SP site; Figure 1b). These contrasting precipitation regimes also influence different ecohydrological responses among water-limited ecosystems and can be used to test how physical forcing factors regulate ET dynamics [*Loik et al.*, 2004; *Scott et al.*, 2012].

In this study, we analyzed ET measured by the eddy covariance technique [*Burba*, 2013] from two water-limited shrublands for the years 2008–2010. One site has WP located in the Diegan xeric Mediterranean climate shrubland [*Westman*, 1983], and the other site is a SP subtropical shrubland located in the southern domain of the NAM [*Méndez-Barroso et al.*, 2014]. Both sites have similar solar radiation patterns (maximum during summer and minimum at winter), are located in the northwest part of Mexico, and are part of the MexFlux network, the eddy covariance network of Mexico [*Vargas et al.*, 2012a, 2013b]. The region of the study sites corresponds to the biome desert and xeric shrublands [*Olson et al.*, 2001], has a high degree of vegetation seasonality [*Forzieri et al.*, 2011], and is considered a climate change hot spot in North America [*Diffenbaugh et al.*, 2008].

Here we ask the following questions: (1) How precipitation variability influences ET at annual and seasonal scales between two water-limited shrublands with different precipitation seasonality but with similar solar radiation-temperature patterns? (2) How the relationship among physical forcing variables (i.e., temperature, radiation, vapor pressure deficit, and soil water content) and ET change among years and seasons at each study site? We postulate two main hypotheses:

1. H1. Intra-annual and interannual variability of ET will be more sensitive to changes in precipitation at the SP site than at the WP site. We postulate this hypothesis because at the WP site the rainy season is longer and therefore is influenced by a larger radiation-temperature gradient that could buffer climatic effects on intra-annual and interannual variability of ET [*Detto et al.*, 2006; *Ryu et al.*, 2008]. In contrast, the SP site is dominated by a short rainy season with a defined radiation-temperature gradient characteristic of the NAM (Figure 1b) that strongly influences ET [*Kurc and Small*, 2004; *Dominguez et al.*, 2008; *Perez-Ruiz et al.*, 2010].
2. H2. Soil water content should be the main control of ET in these water-limited shrublands, as this is the prevailing paradigm in water-limited ecosystems. We recognize that this hypothesis is likely to prevail at the SP site due to distinct precipitation patterns and available energy (i.e., high temperature and high solar radiation) driven by the NAM during the summer months [*Vivoni et al.*, 2008]. In contrast, this hypothesis may not prevail at the WP site where there is a decoupling between precipitation and available energy (i.e., radiation and temperature) and has a longer rainy season characteristic of Mediterranean ecosystems [*Rana and Katerji*, 2000].

The novelty of this study is that these hypotheses have not been simultaneously tested across sites at similar latitudes that are influenced by similar regional climate patterns [*Arriaga-Ramírez and Cavazos*, 2010] but with different timing of precipitation. Finally, this study represents the first collaborative effort toward syntheses studies across the MexFlux network [*Vargas et al.*, 2012a, 2013b].

2. Materials and Methods

2.1. Study Sites

Here we present six site years of information (between 2008 and 2010) from two water-limited sites of the MexFlux network [*Vargas et al.*, 2012a, 2013b]. These sites are characterized by semiarid climates with contrasting precipitation patterns, allowing us to analyze ET under different scenarios of water availability but with similar radiation-temperature patterns.

El Mogor (a site dominated by winter precipitation, hence WP site) is a shrubland located at 406 m above sea level (asl) at the Valle de Guadalupe, Baja California, Mexico (32.03017°N and 116.604219°W) about 30 km from the Pacific Ocean, and it corresponds to the Diegan xeric Mediterranean shrubland association [*Westman*, 1983]. This site has a Mediterranean climate with hot-dry summers and cool-wet winters. The mean annual temperature is 17°C, and the mean annual precipitation is 309 mm yr^{-1}, calculated between 1980 and 2009 (www.daymet.

ornl.gov); rainfall occurs during the cool-wet winters (November–April) with a range of monthly temperatures of 11–14°C and monthly precipitation of 18–63 mm. The warm-dry months (May–October) have a range of monthly temperature of 16–21°C and monthly precipitation between 1 and 6 mm (Figure 1a).

This shrubland is characteristic of a mix chaparral with less sclerophyllous plant species that are characteristic of the Mediterranean chaparral along the coast of California and Baja California. The species with the greatest ground cover at the study site are the following: *Adenostoma fasciculatum*, *Ornithostaphylos oppositifolia*, *Cneoridium dumosum*, *Salvia apiana*, and *Lotus scoparius*. In 2012, the mean canopy height was 1 m. Maximum leaf area index during the years 2011–2012 was 2.15 recorded in March measured with a LI-2200 (LI-COR, Lincoln, NE) [*Leon et al.*, 2014]. The site was severely burned in 1988 and has rapidly recovered in the following 24 years; wildfires are an expected feature of the natural cycle of chaparral [*Franco-Vizcaíno and Sosa-Ramirez*, 1997; *Keeley and Fotheringham*, 2010]. Soils are shallow (nearly 30 cm depth) classified as a typical haploxerolls developed from granitic parent material. Soil texture is sandy loam (i.e., 75% sand, 14% silt, and 11% clay) with a bulk density of 0.93 g cm^3 and pH between 6.6 and 7.0, with a 5% soil carbon, 0.9% soil nitrogen, and a fine root biomass of 0.5 kg m^2 [*Leon et al.*, 2014].

Rayon (a site dominated by summer precipitation, hence SP site) is located at 632 m asl at the edge of the Sierra Madre Occidental 4 km northeast of the town of Rayon in Sonora, Mexico (29.741°N and 110.5337°W). This site has a hot-dry climate, with hot-wet summers and cool winters; the mean annual temperature is 21°C, and the mean annual precipitation is 487 mm yr^{-1}, calculated between 1961 and 2009 (Figure 1b). The study site is within the core of the North American Monsoon System at its southern domain [*Méndez-Barroso et al.*, 2014] region, and therefore, most of the rainfall occurs between the months of July and September (60–70%), with a range of monthly temperatures of 27–30°C and monthly precipitation of 60–125 mm. Meanwhile, the dry months (October–June) have a range of monthly temperatures of 12.5–30°C and monthly precipitation between 5 and <50 mm (Figure 1b).

The species with the greatest ground cover at this subtropical shrubland are the following: *Fouquieria macdougalii*, *Parkinsonia praecox*, *Acacia cochiacanta*, *Jatropha cordata*, and *Encelia farinosa*. In 2012, the mean canopy height was 5 m, and the site has been moderately grazed. The soil depth is ~70 cm, classified as Regosol-Yermosol, and soil texture is silt clay loam (i.e., 56% sand, 10% silt, and 34% clay) with a bulk density of 1.4 g/cm^3. Detailed information about the study site is available in previous studies [*Watts et al.*, 2007; *Vivoni et al.*, 2010a, 2010b; *Tang et al.*, 2012; *Méndez-Barroso et al.*, 2014].

2.2. Instrumentation and Data Acquisition

Each site was instrumented with an eddy covariance tower and an array of meteorological sensors. The flux measurement system at the WP site consisted of an open-path infrared gas analyzer (IRGA; LI-7500, LI-COR, Lincoln, USA) and a three-dimensional sonic anemometer (81000 V, Young, Traverse City, USA) located at 3.5 m above the ground level. Flux measurements were recorded at 20 Hz, and data acquisition was performed by a box computer WaySmall 200ax (Gumstix, Redwood City, USA) during 2008 and subsequently replaced by a Gumstix Verdex on 2009; both computers run in a Linux operating system and an in-house software for data acquisition. Additional meteorological measurements included air temperature and relative humidity (T_a and R_h; HMP-45c, Vaisala, Helsinki, Finland), net radiation (R_n; NR Lite2, Kipp & Zonen, Delft, the Netherlands), photosynthetic photon flux density (PAR Lite, Kipp & Zonen, Delft, the Netherlands), precipitation (P; TR-52USW, Texas Electronic, Dallas, TX, USA), barometric pressure (PTB110, Vaisala, Helsinki, Finland), soil heat flux at 8 cm depth (HFP01, Hukseflux, Delft, the Netherlands), and volumetric soil water content (SWC) using time domain reflectometers at 5, 10, 20, and 40 cm depth (CS616-L, Campbell Scientific, Logan, USA). All meteorological measurements were measured and recorded at a frequency of 1 min. We calculated vapor pressure deficit (VPD) using measurements of T_a and R_h following standard procedures at both sites [*Murray*, 1967].

Instrument calibration was performed on a monthly basis at the WP site as part of quality assurance and quality control protocols [*Foken and Wichura*, 1996].

The SP site is instrumented with a 9 m high T45 tower supporting an eddy covariance system and a suite of meteorological sensors. Flux measurements were carried at the top of the tower with an open-path infrared gas analyzer (IRGA, LI-7500, LI-COR) and a three-dimensional sonic anemometer (CSAT 3, Campbell Scientific); measurements were recorded at 20 Hz. In addition, an anemometer (R. M. Young Co., Traverse City, MI), a temperature-relative humidity probe (HMP45D, Vaisala), and net radiation (CNR-1, Kipp & Zonen,

the Netherlands) sensor were mounted at a height of 7.5 m. A tipping bucket rain gauge (TR-52USW) was installed at 1.5 m high in an open area. Soil heat flux was measured using two soil plates at 3 cm depth (HFP01SC, Hukseflux). Soil moisture was measured at 5 and 10 cm depth with soil water content reflectometers (CS616-L). All meteorological variables were measured at 1 min, while the 30 min averages were stored.

2.3. Data Processing and Gap Filling

Raw flux data were processed to half-hourly averages using the eddy covariance software EddyPro version 4 (LI-COR), which includes conventional corrections for calculating eddy covariance measurements [*Burba*, 2013]. Statistical outliers for all micrometeorological measurements outside the ±3 SD range of a 14 day running mean window were removed. Periods with low turbulence conditions were excluded based on friction velocity ($u*$). We determined seasonal and site-dependent $u*$ thresholds according to quantitative methods [*Gu et al.*, 2005]. At the WP site, this algorithm yielded $u* = 0.10\,\mathrm{m\,s^{-1}}$ for the three years analyzed, and for the SP site $u* = 0.17\,\mathrm{m\,s^{-1}}$ for 2008, $u* = 0.16\,\mathrm{m\,s^{-1}}$ for 2009, and $0.16\,\mathrm{m\,s^{-1}}$ for 2010. After $u*$ quality filtering, which mostly occurs at night, 62% of the data remained for the WP site and 57% for SP site. Storage fluxes were not calculated because the study sites have short canopy with well mixing and we assumed the storage flux to be zero for a 24 h period.

Using filtered data, we calculated the energy balance closure as an independent measure to evaluate the performance of eddy covariance measurements following standardized guidelines [*Wilson et al.*, 2002]. Ground heat flux was derived from three soil heat flux plates at the WP site and from two soil heat flux plates at the SP site. The energy balance closure was only calculated for the periods when data for all components (LE, H, G, and R_n) were available. Energy balance closure was evaluated for each site using the energy balance ratio defined as the cumulative sums using the daily values for the total study period of turbulent fluxes (LE + H) divided by the available energy ($R_n - G$). Energy balance closure for the WP site was 0.82 and for SP site was 0.89 for the years 2008 to 2010. These reports are in accordance with Fluxnet open and closed shrublands that have a mean of 0.87 ± 0.15 [*Stoy et al.*, 2013].

For all data analyses we used filtered data (i.e., data with gaps), but for comparing annual sums and performing time series analyses we used gap-filled time series. Data gaps were filled following the procedures by the online eddy covariance gap-filling and flux-partitioning tool available at http://www.bgc-jena.mpg.de/~MDIwork/eddyproc/ [*Reichstein et al.*, 2005].

2.4. Definition of Seasons and Transitions of Seasons

In order to determine interannual variability at both sites, we defined wet and dry seasons and the transitions between them (e.g., wet-dry and dry-wet) following a simple combination of precipitation (P) events and soil water content (SWC) at each site. It has been reported that P events of 5 mm are enough to trigger ET responses across water-limited ecosystems of North America [*Schwinning and Sala*, 2004]. We defined the start of the wet season after the first rainfall event ≥5 mm only if it was followed by another ≥5 mm P event within the next 25 days. We defined the dry season after the last rainfall event ≥5 mm and if that event was not followed by another ≥5 mm P event within the next 25 days.

In water-limited ecosystems, ET is largely constrained by water availability [*Lauenroth and Bradford*, 2009], so we also classified the transitions between seasons using SWC time series. The wet-dry transition started after the beginning of the dry season (defined by P events described above) and continued until the SWC decreased to the mean value of SWC during the dry season. The dry-wet transition started after the beginning of the wet season and continued until the SWC increased to the mean value of SWC during wet season. Finally, we compiled the length of the dry season by removing the days of the wet-dry transition, and we compiled the length of the wet season by removing the days of the dry-wet transition. Using this approach, we ended with unique days for the dry and wet seasons and the dry-wet and wet-dry transitions for each year at each study site.

2.5. Data Analyses

We used one-way analysis of variances (ANOVAs) to determine differences in ET between years or among seasons at each study site. A Tukey post hoc test was used to determine differences among years or seasons if the ANOVA test showed significant differences [*Bennington and Thayne*, 2014].

We explored the spectral properties of the half-hourly resolution of the ET time series using the continuous wavelet transform at both study sites. Previous studies have reviewed in detail the concept of wavelet

analysis [*Torrence and Compo*, 1998], and it has been extensively used for analysis of ecosystem-scale fluxes [*Stoy et al.*, 2009; *Ding et al.*, 2013], soil CO_2 efflux research [*Vargas et al.*, 2010], and data-model comparisons [*Dietze et al.*, 2011; *Vargas et al.*, 2013b]. Briefly, this technique provides information about the periodicities of the time series and allows us to identify the relevant frequencies and differences in the spectral properties of time series. For this analysis, we used the Morlet mother wavelet, which is a complex nonorthogonal wavelet used commonly in geophysical applications [*Torrence and Compo*, 1998]. To analyze the data, we first normalized the gap-filled time series of observations by:

$$ET' = \frac{(ET - mean(ET))}{std(ET)} \tag{1}$$

where *ET'* is the ET normalized at 30 min average and ET is the original gap-filled time series at 30 min. Then, we calculated the global power spectra using the continuous wavelet transform for each normalized time series of ET (i.e., *ET'*).

We explored the temporal correlation between ET and air temperature (T_a) using wavelet coherence analysis (WCA) [*Grinsted et al.*, 2004]. Previous studies have described the technique in detail for climate studies [*Torrence and Compo*, 1998; *Grinsted et al.*, 2004], micrometeorological measurements [*Vargas et al.*, 2011], and evapotranspiration at the ecosystem scale [*Ding et al.*, 2013]. Briefly, coherency is roughly similar to classical correlation, but it pertains to the oscillating components in a given time period (e.g., 1 day and 16 days). Therefore, we can identify time periods with high temporal correlations between two original time series. Here we combined the information from *P* and T_a (at each study site) using principal component analysis (PCA), and we used the first principal component (i.e., PC1) to explore its temporal correlation with ET at each study site. This approach summarizes the potential temporal correlations between temperature and *P* with ET rather than performing individual WCA for each variable with ET at each study site.

We applied regression tree analysis to identify how predictor variables influenced the magnitude of ET across years and among seasons [*Breiman et al.*, 1984]. We used the daily mean values of ET (as a response variable), and we used soil water content (SWC), net radiation (R_n), air temperature (T_a), and vapor pressure deficit (VPD) as predictor variables. Regression tree analysis partitions the data into two clusters, optimizing the use of predictor variables to best classify the response (i.e., ET). The process is repeated on each cluster until a significant partition cannot be made of the remaining variance. We used a minimum node of size 3, meaning no node with fewer than three data points was split. The advantage of this method is that the tree structure enables a hierarchical interpretation of the importance of the independent variables as done for other micrometeorological applications [*Vargas et al.*, 2010]. Individual regression tree analyses were performed of each season (i.e., wet and dry) and their transitions (i.e., wet-dry and dry-wet) for each site to predict ET. All data were processed in MATLAB 7.4, R2007a (MathWorks, Natick, Massachusetts, USA).

3. Results

3.1. Annual Dynamics of Physical Forcing Variables and ET

The WP site had high ET (up to $3.0\ mm\ d^{-1}$) and soil moisture (SWC, $0.19\ m^3\ m^{-3}$ mean value of the three wet seasons) when net radiation (R_n, $36\ W\ m^{-2}$ mean value of the three wet seasons) and temperature (T_a; 11°C mean value of the three wet seasons) were low (Figure 2). In contrast, the SP site had high ET (up to $5.8\ mm\ d^{-1}$) and SWC ($0.11\ m\ m^{-3}$, mean value of the three wet seasons) when R_n ($151\ W\ m^{-2}$ mean value of the three wet seasons) and T_a (28° C, mean value of the three wet seasons) were also high (Figure 2). At the WP site, the mean annual *P* for the entire study was $341\ mm\ yr^{-1}$, the daily mean R_n was $74 \pm 58\ W\ m^{-2}\ d^{-1}$ (± 1 standard deviation), the daily mean T_a was 15 ± 6°C, the daily mean SWC was $0.13 \pm 0.06\ m^3\ m^{-3}$ at 5 cm depth, and the mean annual VPD was 0.91 ± 0.3 kPa. The SP site had a mean annual *P* of $493\ mm\ yr^{-1}$, the daily mean R_n was $110 \pm 58\ W\ m^{-2}\ d^{-1}$, the daily mean T_a was 23 ± 6°C, the daily mean SWC was $0.06 \pm 0.06\ m^3\ m^{-3}$ at 5 cm depth, and the mean annual VPD was 2.00 ± 0.9 kPa across the three years. The WP site had a mean annual daily ET of $1.10 \pm 0.60\ mm\ d^{-1}$, whereas the SP had a mean annual daily ET of $1.38 \pm 1.46\ mm\ d^{-1}$.

3.2. Time Series Analyses of ET

The ET time series at the WP site showed a weak spectral power at 1 day and a strong peak at 1 year with a spectral gap between them (Figure 3a). We found a weak spectral power at 1 day and strong spectral power at 1 year and ~150 days at the SP site (Figure 3b).
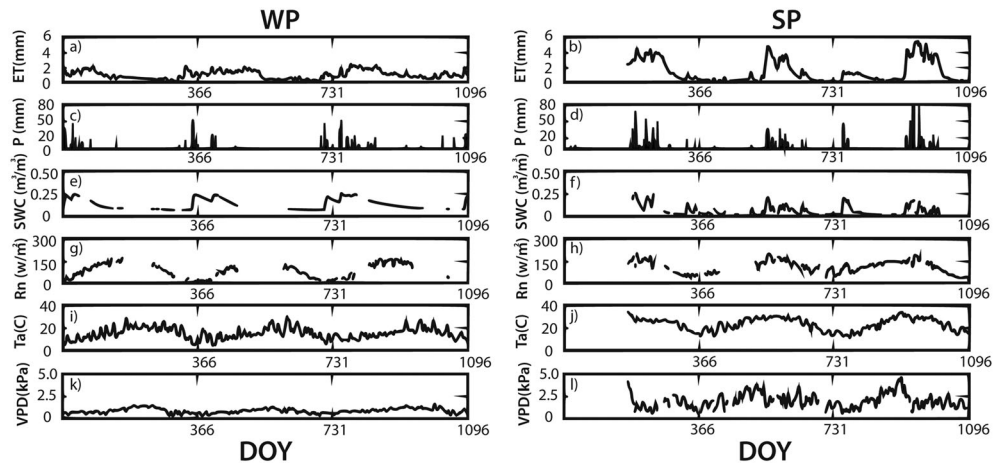
Figure 2. Daily average of (a, b) evapotranspiration, (c, d) precipitation, (e, f) soil moisture, (g, h) net radiation, (i, j) temperature, and (k, l) vapor pressure deficit between 2008 and 2010 for the winter precipitation (WP) and summer precipitation site (SP), respectively.

We performed WCA using daily values of P, T_a, and ET. First, we perform a PCA using P and T_a at each study site. We found that the first principal component (i.e., PC1) explained 65% of the variance for P and T_a at the WP site (Figure 4a) and was negatively correlated with P (-0.57) and positively correlated with T_a (0.82). The PC1 at the SP site (Figure 4b) explained 60% of the variance and was strongly positively correlated with P (0.99) and weakly positively correlated with T_a (0.17). Second, we applied WCA on the PC1 and ET time series for each study site. The WCA shows that for the WP site there is significant temporal correlation (i.e., red areas in Figure 4a) at time periods over 256 days, but there is no consistency in the temporal correlations at lower time periods. In contrast, the WCA shows that at the SP site (Figure 4b) PC1 and ET have significant temporal correlations in time periods between 16 and over 256 days. Furthermore, the majority of the time periods with significant temporal correlation for the SP site show that PC1 and ET are in phase (i.e., arrows pointing to the right) demonstrating the high dependency on P patterns at this study site.

3.3. Annual Variations of ET

At the WP site we had one year with low P (i.e., 2009), an average year (i.e., 2008), and a year with high P (i.e., 2010, Table 1). Annual ET was significantly higher (423 mm yr^{-1}; ANOVA; $F = 22.33$, $P < 0.001$) during 2010,
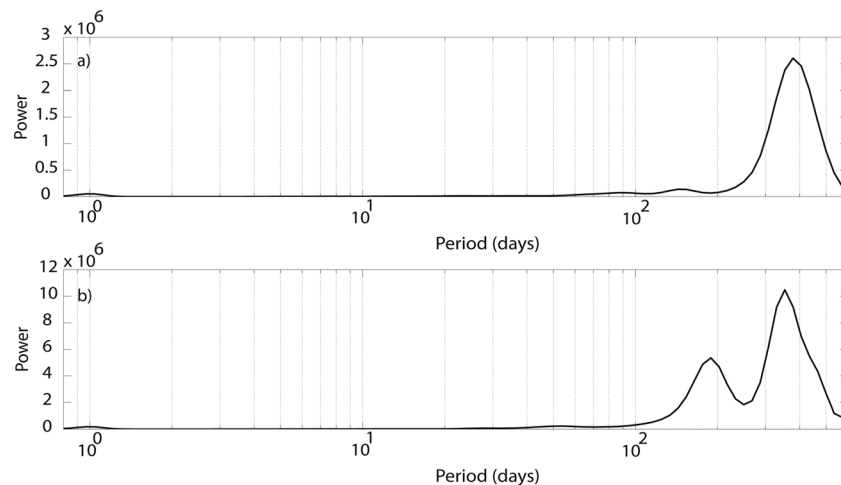

Figure 3. Wavelet power spectra of the time series of evapotranspiration (ET) at the (a) winter precipitation (WP) and (b) summer precipitation (SP) sites. Sites show spectral density at 1 day, ~150 day, and 365 day periods that correspond to daily, seasonal, and annual time scales.
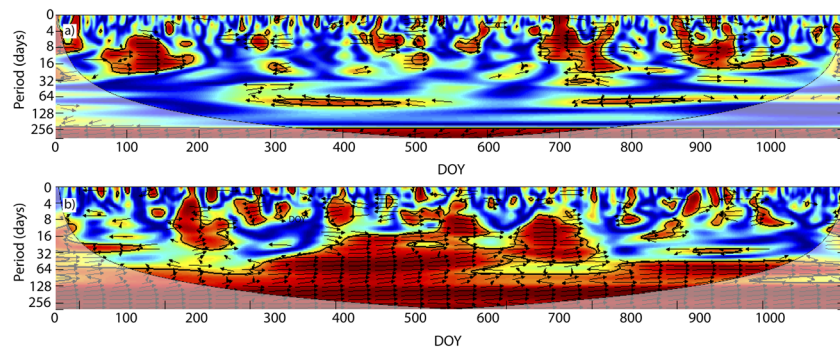
Figure 4. Wavelet coherence analysis and phase difference between evapotranspiration (ET) and precipitation and air temperature at the (a) winter precipitation (WP) and (b) summer precipitation (SP) sites for the years 2008–2010. The variability of the times series of precipitation and air temperature was summarized using the first principal component of a principal component analysis (PCA; see section 2). Arrows show the phase differences: in-phase pointing right (no lags between time series) and out of phase pointing in other direction (representing lags between time series). The color codes for power values are from dark blue (low values) to dark red (high values). Black contour lines represent the 5% significance level, and thick black line indicates the cone of influence that delimits the region not influenced by edge effects. DOY, day of the year after 1 January 2008.

but no significant differences were found during 2008 and 2009 (327 and 339 mm yr^{-1}, respectively; Table 1 and Figure 5a). The annual difference between daily P and daily ET was relatively similar between 2008 and 2010 (71 and 62 mm yr^{-1}), but there was a substantial deficit for the dry year of 2009 (-119 mm yr^{-1}). Noteworthy, this deficit was not related with a decline in annual ET for the year 2009 (Figure 5b). Despite the large differences in P among the years, seasonal magnitudes and trends of VPD were similar among the years (Figure 5c).

At the SP site annual P was relatively similar for 2008 and 2010 (Table 1) and substantially lower for 2009 (i.e., dry year). Noteworthy, we found more extreme rainfall events (i.e., individual events >3 standard deviations) during 2010 than 2008. ET was significantly higher (ANOVA; $F = 44.61$, $P < 0.001$) during 2010 (515 mm yr^{-1}, Table 1) and 2008 (499 mm yr^{-1}) when compared to the dry year of 2009 (350 mm yr^{-1}; Table 1 and Figure 5d). The difference between daily P and daily ET was relatively similar between 2008 and 2010 (46 and 40 mm yr^{-1}), but it was significantly lower for the dry year of 2009 (11 mm yr^{-1}; Table 1). Cumulative P-ET followed a step function driven by the dry months and followed by the intense P during the NAM season during the summer months (Figure 5e). In contrast with the WP site, the dry year at the SP site resulted in substantial differences in seasonal trends and magnitudes of VPD (Figure 5f) and therefore annual ET (Figure 5d and Table 1).

Using regression tree analysis, we found that for both sites SWC and R_n were important predictors for ET among the years, but the complexity of the regression trees (i.e., number of variables and clusters in the trees) differed among the years (Figure 6). At the WP site, the most complex tree was for the year with lower annual

Table 1. Characteristics of Annual Precipitation and Evapotranspiration (ET) at the Winter Precipitation (WP) and Summer Precipitation (SP) Sites[a]

Site	Year	Annual Precipitation (mm)	Annual Precipitation Anomaly (mm yr^{-1})	Annual Sum of ET (mm)	Annual Precipitation Minus ET (mm)	Mean Daily ET (mm d^{-1})	Days With ET Lower Than Mean Daily ET	Mean Temperature (°C)
WP	2008	398	109	327	71	0.9 ± 0.5 a	143	15.7 ± 6
	2009	220	−69	339	−119	0.9 ± 0.6 a	168	14.7 ± 5
	2010	485	196	423	62	1.2 ± 0.6 b	145	14.8 ± 5
SP	2008	545	58	499	46	2.1 ± 1.4 A	102	24.3 ± 4
	2009	361	−126	350	11	0.9 ± 1.2 B	100	23.9 ± 5
	2010	556	69	515	41	1.4 ± 1.5 C	109	22.5 ± 6

[a]Different letters show significant differences ($P < 0.001$) following a Tukey *post hoc* test.
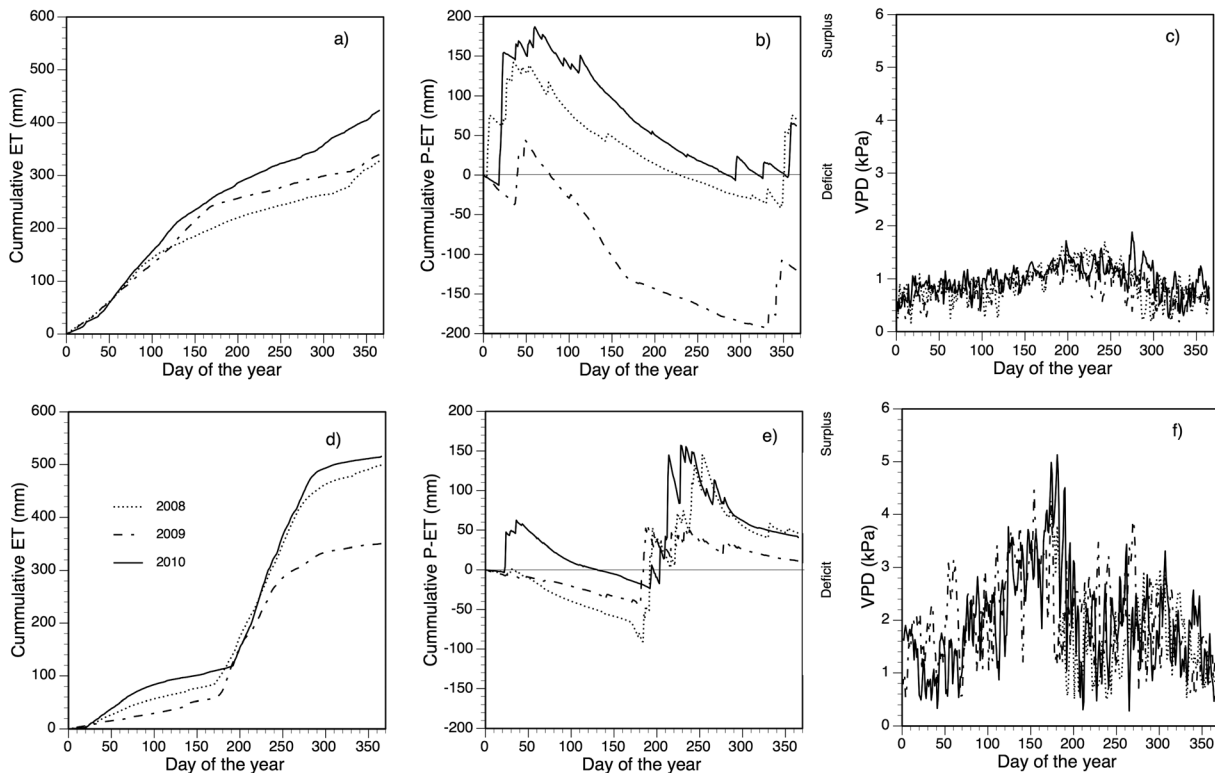
Figure 5. Cumulative (a, d) daily evapotranspiration (ET), (b, e) daily water deficit (P minus ET), and (c, f) daily vapor pressure deficit (VPD) along the different studied years at the winter precipitation (WP; Figures 5a–5c) and summer precipitation (SP; Figures 5d–5f) sites. DOY, day of the year after 1 January for each year.

P (i.e., 2009; Figures 6b and 6e) and years with higher annual P had regression trees with less clusters. The complexity of regression trees at the SP site followed a different pattern. For the drier (i.e., 2009) and average P year (i.e., 2008), the complexity of the regression trees was lower (Figures 6j and 6k). For the year with the highest annual P, we found the most complex regression tree (Figures 6i and 6l), where SWC, R_n, and T_a were important to explain ET. The fit of the annual regression trees was lower for the SP site (r^2 between 0.37 and 0.78) compared with the WP site (r^2 between 0.64 and 0.78; Figure 6).

3.4. Seasonal Variation of ET

Both sites were characterized by a long dry season (55% of days for the WP site and 75% for the SP site), but the WP site had more days with available water (i.e., combination of wet plus wet-dry with a total of 42% of days; Table 2). Mean daily ET was relatively constant for the WP site, but with a significant reduction during the dry season (ANOVA; $F = 128.62$, $P < 0.00$; Table 2). In contrast, mean daily ET was substantially higher during the dry-wet and wet seasons at the SP site but significantly lower during the dry season (ANOVA; $F = 1354.61$, $P < 0.001$; Table 2).

For both sites, daily R_n and SWC were the main physical forcing variables to explain daily ET among seasons (Figures 7b and 7f). During the wet season, R_n was the main variable for explaining high ET at the WP site and SP site; however, R_n is considerably higher at the SP site ($R_n = 151$ W m^{-2}) than at the WP site ($R_n = 36$ W m^{-2}). During the dry season, SWC was the main physical forcing variable at both sites (Figures 7c and 7g). During the wet-dry transition, SWC was the main physical forcing variable followed by T_a at the WP site, but only T_a was significant for the SP site (Figures 7d and 7h). For the dry-wet transition, we did not find a significant regression tree for the WP site suggesting larger variability to explain ET for this transition phase; however, R_n was the main physical forcing variable followed by VPD at the SP site (Figure 7i). These analyses show that simpler regression trees describe daily ET for almost all seasons at the SP site, but more complex trees were needed to explain ET at the WP site. The fit (r^2) of the seasonal regression trees for the SP site was between 0.23 and 0.88 and for the WP site was between: 0.32 and 0.62 (Figure 7).
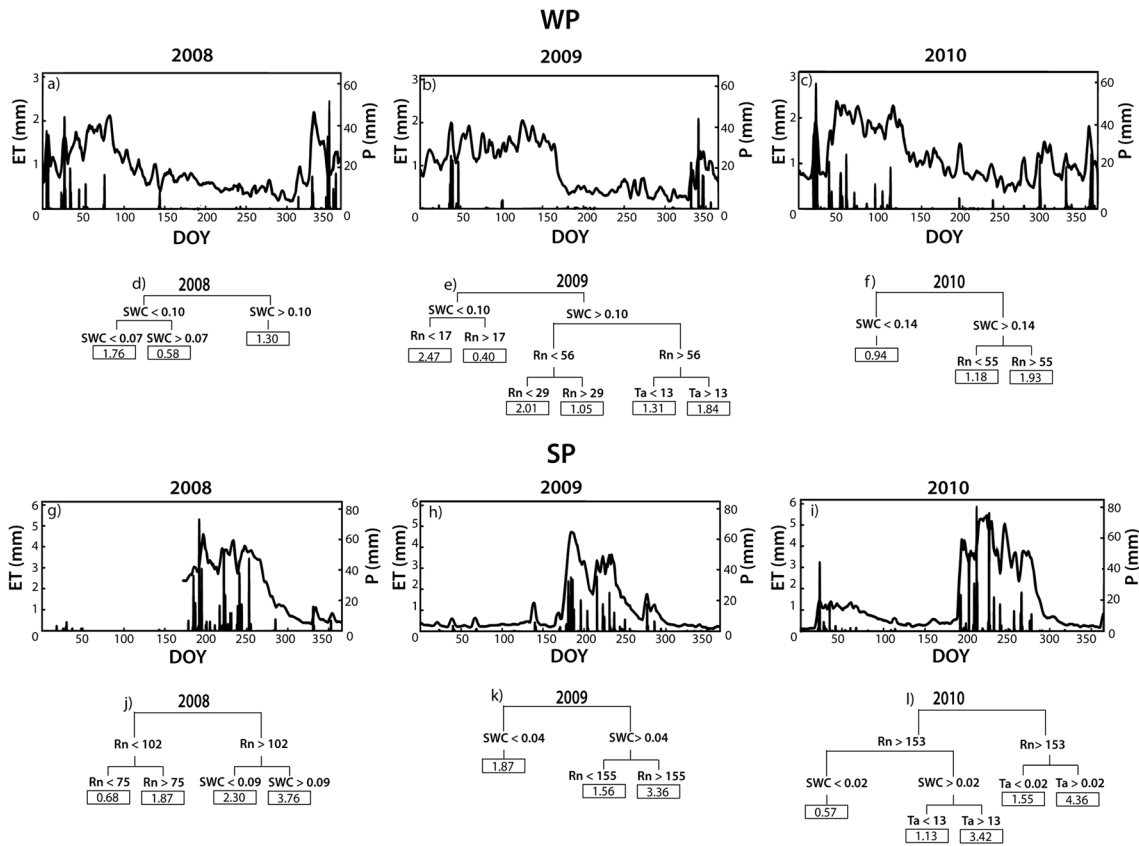
Figure 6. Annual mean daily precipitation and evapotranspiration (ET) patterns at (a–c) winter precipitation (WP) and (g–i) summer precipitation (SP) sites. Regression tree analyses showing the main physical forcing variables influencing ET at (d–f) WP and (j–l) SP sites.

4. Discussion

Our results support H1, as we observed that ET at the WP site is less sensitive to annual rainfall variability and to seasonal variability as compared to the SP site. Despite large changes in annual P, annual sum of ET was relatively constant at the WP site, but highly variable at the SP site. Our results do not fully support H2 because although SWC is the main control of ET at the SP site, we found evidence that multiple forcing variables control ET when precipitation is decoupled from available energy at the WP site.

4.1. Time Series Analyses of ET Between Sites

Due to contrasting P seasonality, available energy, and plant phenology between sites, the SP site had a stronger seasonal (~150 days) ET spectral density compared to the WP site. This is explained by the prolonged but variable rainy season (November to March) in southern California and northern Baja California [*Nezlin and Stein*, 2005] that results in a low spectral density at the seasonal scale as observed in other water-limited

Table 2. Seasonal Characteristics of Evapotranspiration (ET) at the Study Sites With Winter Precipitation (WP) and Summer Precipitation (SP)[a]

Site	Season	Percent Days	Percent of Annual Precipitation	Percent of Annual ET	Mean Daily ET (mm d^{-1})	Mean Temperature (°C)
WP	Wet	31	80	40	1.3 ± 0.6 a	11.1 ± 4
	Wet-dry	11	4	15	1.4 ± 0.4 a	13.4 ± 0.1
	Dry	55	9	40	0.7 ± 0.4 b	17.9 ± 5
	Dry-wet	3	7	5	1.2 ± 0.7 a	11.1 ± 4
SP	Wet	20	56	52	3.5 ± 1.1 A	27.8 ± 2
	Wet-dry	3	2	18	2.2 ± 1.1 B	24.1 ± 3
	Dry	75	25	25	0.4 ± 0.4 C	21.7 ± 6
	Dry-wet	2	17	5	3.6 ± 1.0 A	29.4 ± 3

[a]Different letters show significant differences ($P < 0.001$) following a Tukey *post hoc* test.
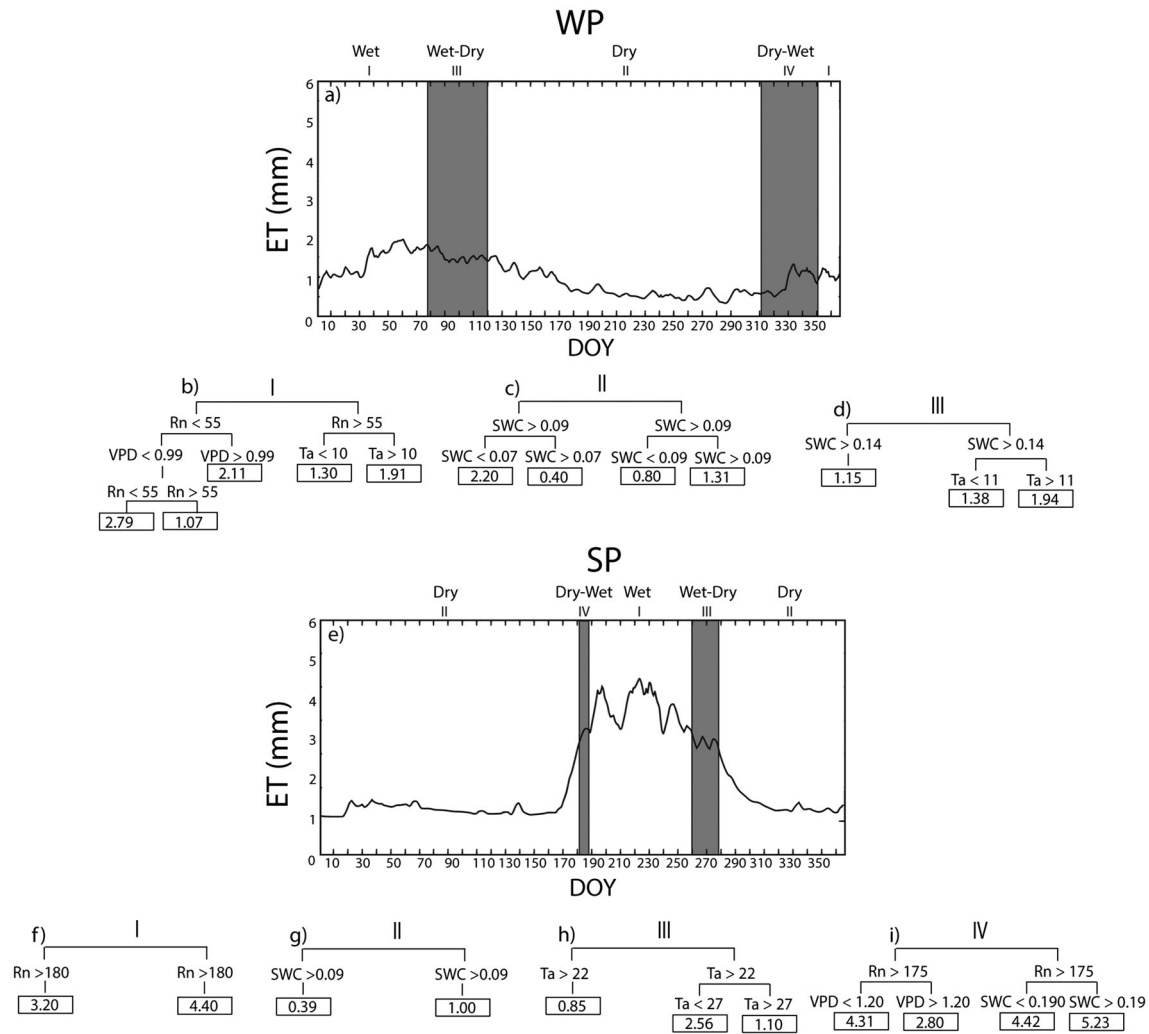
Figure 7. Multiannual average of evapotranspiration (ET) at (a) winter precipitation (WP) and (e) summer precipitation (SP) sites. Regression tree analyses showing the main physical forcing variables influencing ET at a seasonal scale for the wet season at (b) WP and (f) SP, dry season at (c) WP and (g) SP, wet-dry transition at (d) WP and (h) SP, and dry-wet transition at (i) SP.

ecosystems [*Vargas et al.*, 2013a]. In contrast, the SP site showed a strong seasonal (~150 days) ET spectral density due to the influence of the NAM on ET. Arguably, ET could be easily predicted for the SP site that has a defined seasonality and spectral signature that is coupled with phenology (Figure 1). Finally, both sites showed weak spectral density at the 1 day period that is overshadowed by the synoptic patterns at ~150 and 365 days. Also, during the prolonged dry season the diel pattern of ET is not persistent at both sites (due to water limitation and low plant metabolism) therefore dampening the spectral signal at the 1 day period in the global power spectra. This result contrasts with observations at sites subject to P evenly distributed over the year and irrigated sites where there is a strong diel pattern (i.e., 1 day period) in ET [*Ding et al.*, 2013].

The wavelet coherence analysis (WCA) showed that ET at the SP site has strong and consistent temporal coherency (between 32 and 365 days) with T_a and P. Precipitation and T_a are positively correlated (see PC1 results for SP site) and demonstrate the coupling between available water and temperature during the NAM. The importance of the NAM on ET in water-limited ecosystems of northern Mexico and Southwest of the United States have been described previously [*Kurc and Small*, 2004; *Vivoni et al.*, 2010b; *Scott et al.*, 2012; *Méndez-Barroso et al.*, 2014], and changes in the intensity of the NAM could substantially reduce the annual fluxes of ET [*Tang et al.*, 2012] (Figure 4). Thus, our analysis supports the paradigm that there is strong temporal coupling between water and temperature for controlling ET dynamics when available energy is not a limiting factor (see H2). In contrast, P and T_a are negatively correlated at the WP site (see PC1 results) and

demonstrate the decoupling between available water and temperature in Mediterranean ecosystems. Furthermore, the WCA shows that there is a weak temporal coherency between ET with T_a and P demonstrating that the temporal dynamics of ET are dependent on variables beyond T_a and P at the SP site.

4.2. Annual Variability of ET

This study provided an excellent opportunity to compare ecosystem water deficit (i.e., P-ET) and to analyze how ET dynamics respond to normal annual precipitation (year 2008), drought (year 2009), and higher than normal (year 2010) precipitation across sites with different precipitation regimes. Precipitation deficits during 2009 resulted in water deficits (i.e., negative P-ET), while the wet year presented a positive P-ET in both of these water-limited ecosystems.

At the SP site, ET is tightly coupled with P, and ET is highly sensitive to changes in annual P. For the drier and normal P year, ET is controlled only by R_n and SWC, as is expected for a traditional water-limited ecosystem [*Porporato et al.*, 2002]. However, as the environment becomes wetter, T_a also becomes a significant forcing factor on ET, suggesting the direct relation between water availability and vegetation metabolism for the SP site [*Vivoni et al.*, 2010b; *Méndez-Barroso et al.*, 2014] (Figure 6). These results provide evidence that changes in the intensity and frequency of P driven by the NAM could substantially influence annual ET fluxes across north central Mexico and southwestern United States [*Perez-Ruiz et al.*, 2010; *Méndez-Barroso et al.*, 2014].

In contrast, a reduction in annual P at the WP site resulted in large water deficits, but annual ET was not substantially changed among the years (Figure 5). One possible explanation to compensate for the water deficit is the influence of fog transported inland from the ocean [*Corbin et al.*, 2005; *Estrela et al.*, 2009] keeping VPD relatively constant even during drought years (Figure 5). This is likely a result of the increased thermal contrast between the land and ocean during dry and hot years that enhance a positive feedback that transport fog into the land during upwelling events in the coastal ocean [*Olivier*, 2004]. Similar teleconnection patterns and the influence of fog in sites dominated by winter P have been reported previously [*Olivier*, 2004; *Agam and Berliner*, 2006; *Kalthoff et al.*, 2006] and across Baja California [*Reimer et al.*, 2015]. During the wet and normal precipitation years, annual ET is only influence by R_n and SWC as is expected for a traditional water-limited ecosystem [*Porporato et al.*, 2002]. In contrast, the driest year needed a more complex regression tree to explain the relatively high ET likely as a potential result of lateral transport of moisture from the ocean to the land in this coastal ecosystem [*Reimer et al.*, 2015] (Figure 6).

4.3. Seasonal Variability of ET

The contrasting precipitation patterns between the study sites offered an excellent opportunity to test how precipitation regimes and energy availability influence seasonal ET between these water-limited ecosystems. When water is available, nearly 40% of total ET fluxes occurred at the WP site (wet winter months; Table 2) and nearly 52% at the SP site (wet summer months; Table 2). At the WP site, the scattered rains and low R_n-T_a limits ET during winter and leads to a relatively high water availability (SWC; Figure 2) where plants grow and gross primary production is relatively high as seen at other Mediterranean ecosystems [*Serrano-Ortiz et al.*, 2007; *Domingo et al.*, 2011]. These wet conditions associated with low radiation-temperature regime allow a complex relation between the physical forcing variables (i.e., R_n, T_a, and VPD; Figure 7). Thus, these results highlight the role of R_n-T_a in water-limited ecosystems as a limiting factor for ET and other biogeo-chemical cycles (e.g., carbon fluxes) [*Rana and Katerji*, 2000], when P is available during the winter season.

The seasonal ET transitions (e.g., wet-dry and dry seasons) are characterized by rapid changes in the radiation-temperature regimes and water availability at the studied sites. Importantly, the intensity and frequency of precipitation along with the radiation-temperature regime controls the length (and the influence of forcing factors on ET) of the ET transitions at the study sites. At the WP site, the wet-dry transition has the highest daily ET fluxes among seasons (Table 1). These high daily ET fluxes can be explain by the relatively high available SWC and by an increase in the radiation-temperature regime, as seen in other water-limited ecosystems [*Scott et al.*, 2012]. At the SP site, the wet-dry transition is marked by the end of the NAM season, a rapid decline in water availability along with a high radiation-temperature regime [*Méndez-Barroso et al.*, 2014] (Figure 7), resulting in a reduction in daily ET for the SP site (Table 2).

For the dry-wet transition at the WP site, the season was characterized by relatively low daily ET. This could be explained by the relatively low depth and frequency of precipitation pulses in conjunction with low

radiation-temperature regime. Due to rapid changing conditions during this season and low ET responses, we did not find a significant regression tree, suggesting possible stronger nonlinear controls over ET. In contrast, at the WP site the dry-wet transition shows the importance of the magnitude and distribution of precipitation pulses, as plants rapidly use the available resources after the long dry period as seen in other ecosystems influenced by the NAM [*Schwinning and Sala*, 2004; *Méndez-Barroso et al.*, 2014]. During this season, at the SP site, rapid environmental and phenological changes are coupled with the high radiation-temperature regime resulting into a rapid increase in daily ET. It is known that these early rains are critical in water-limited ecosystems and drive many biogeochemical cycles after the long dry season [*Austin et al.*, 2004; *Yepez et al.*, 2007; *Lauenroth and Bradford*, 2009; *Méndez-Barroso et al.*, 2014]. These pulses of ET during the dry-wet transition are explained by changes in R_n and VPD (Figure 7). These results highlight the complexity of forcing factors on ET during unstable weather conditions following the dry months and the challenge for representing these transitions in ecosystem process models [*Vargas et al.*, 2013a].

The relationship between ET and SWC has been largely known [*Wetzel and Chang*, 1987] and has been recognized as an important factor for water-limited ecosystems [*Porporato et al.*, 2002]. Thus, several modeling approaches have incorporated SWC into calculations for representing ET in Mediterranean ecosystems [*Longobardi and Khaertdinova*, 2015] and within the NAM [*Vivoni et al.*, 2008]. Furthermore, other studies have recognized the importance of SWC for plant water uptake within the rooting zone and have modified the widely used Penman-Monteith equation to incorporate SWC to model ET in water-limited regions [*Sun et al.*, 2013]. Our study support these efforts by demonstrating that SWC is the main control of ET when available energy is not a limiting factor, but ET is controlled by an interaction of multiple variables when SWC is decoupled from available energy between water-limited ecosystems.

5. Conclusions

Water-limited ecosystems share several common ecohydrological characteristics, but due to their diversity in vegetation and radiation-temperature regimes, ET dynamics respond differently to seasonal precipitation patterns. Variability of ET in a shrubland where precipitation was coupled with high available energy (i.e., radiation and temperature; SP site) was explained by changes in R_n and SWC. In contrast, variability of ET was difficult to explain in a shrubland where available energy was decoupled from precipitation (WP site). This study highlights several results: (a) the spectral power of ET at both sites showed large spectral densities at 365 days, but there was higher spectral density at ~150 days for the SP site due to rains provided by the NAM; (b) wavelet coherence analysis showed that ET at SP site has strong and consistent temporal coherency with T_a and P, but this was not the case for ET at WP site; (c) the WP site had relatively low annual sums of ET than the semiarid shrubland, likely a result of lower annual precipitation and its decoupling with available energy; (d) both sites experienced a drought year (2009), but the SP site was highly sensitive to reduced annual precipitation; and (e) our results support the paradigm that SWC is the main control of ET in water-limited ecosystems when radiation and temperature are not limiting factors (SP site); when P and SWC are decoupled from available energy, then ET is controlled by an interaction of multiple variables (WP site). Finally, our results bring attention to the range of variables controlling ET across the diversity of water-limited ecosystems, as it cannot be assumed that forcing variables influence ET in the same way across these globally distributed ecosystems.

References

Agam, N., and P. R. Berliner (2006), Dew formation and water vapor adsorption in semi-arid environments—A review, *J. Arid Environ.*, *65*, 572–590, doi:10.1016/j.jaridenv.2005.09.004.

Arriaga-Ramírez, S., and T. Cavazos (2010), Regional trends of daily precipitation indices in northwest Mexico and southwest United States, *J. Geophys. Res.*, *115*, D14111, doi:10.1029/2009JD013248.

Austin, A. T., L. Yahdjian, J. M. Stark, J. Belnap, A. Porporato, U. Norton, D. A. Ravetta, and S. M. Schaeffer (2004), Water pulses and biogeochemical cycles in arid and semiarid ecosystems, *Oecologia*, *141*, 221–235, doi:10.1007/s00442-004-1519-1.

Baldocchi, D., M. Reichstein, D. Papale, L. Koteen, R. Vargas, D. Agarwal, and R. Cook (2012), The role of trace gas flux networks in the biogeosciences, *Eos (Washington. DC)*, *93*(23), 217–224.

Beer, C., et al. (2010), Terrestrial gross carbon dioxide uptake: Global distribution and covariation with climate, *Science*, *329*, 834–838, doi:10.1126/science.1184984.

Bennington, C., and W. Thayne (2014), Use and misuse of mixed model analysis of variance in ecological studies, *Ecology*, *75*(3), 717–722.

Breiman, L., J. Friedman, and R. Olshen (1984), *Classification and Regression Trees*, CRC Press, Boca Raton, Fla.

Burba, G. (2013), *Eddy Covariance Method for Scientific, Industrial, Agricultural and Regulatory Applications: A Field Book on Measuring Ecosystem Gas Exchange and Areal Emission Rates*, Li-Cor Bioscience, Lincoln, Nebraska.

Corbin, J. D., M. A. Thomsen, T. E. Dawson, and C. M. D'Antonio (2005), Summer water use by California coastal prairie grasses: Fog, drought, and community composition, *Oecologia*, *145*, 511–521, doi:10.1007/s00442-005-0152-y.

Detto, M., N. Montaldo, J. D. Albertson, M. Mancini, and G. Katul (2006), Soil moisture and vegetation controls on evapotranspiration in a heterogeneous Mediterranean ecosystem on Sardinia, Italy, *Water Resour. Res.*, *42*, 1–16, doi:10.1029/2005WR004693.

Dietze, M. C., et al. (2011), Characterizing the performance of ecosystem models across time scales: A spectral analysis of the North American Carbon Program site-level synthesis, *J. Geophys. Res.*, *116*, G04029, doi:10.1029/2011JG001661.

Diffenbaugh, N. S., F. Giorgi, and J. S. Pal (2008), Climate change hotspots in the United States, *Geophys. Res. Lett.*, *35*, L16709, doi:10.1029/2008GL035075.

Ding, R., S. Kang, R. Vargas, Y. Zhang, and X. Hao (2013), Multiscale spectral analysis of temporal variability in evapotranspiration over irrigated cropland in an arid region, *Agric. Water Manage.*, *130*, 79–89, doi:10.1016/j.agwat.2013.08.019.

Domingo, F., P. Serrano-Ortiz, A. Were, L. Villagarcía, M. García, D. A. Ramírez, A. S. Kowalski, M. J. Moro, A. Rey, and C. Oyonarte (2011), Carbon and water exchange in semiarid ecosystems in SE Spain, *J. Arid Environ.*, *75*, 1271–1281, doi:10.1016/j.jaridenv.2011.06.018.

Dominguez, F., P. Kumar, and E. R. Vivoni (2008), Precipitation recycling variability and ecoclimatological stability—A study using NARR data. Part II: North American monsoon region, *J. Clim.*, *21*(20), 5187–5203, doi:10.1175/2008JCLI1760.1.

Estrela, M. J., J. A. Valiente, D. Corell, D. Fuentes, and A. Valdecantos (2009), Prospective use of collected fog water in the restoration of degraded burned areas under dry Mediterranean conditions, *Agric. For. Meteorol.*, *149*, 1896–1906, doi:10.1016/j.agrformet.2009.06.016.

Foken, T., and B. Wichura (1996), Tools for quality assessment of surface-based flux measurements, *Agric. For. Meteorol.*, *78*(1–2), 83–105, doi:10.1016/0168-1923(95)02248-1.

Forzieri, G., F. Castelli, and E. R. Vivoni (2011), Vegetation dynamics within the North American monsoon region, *J. Clim.*, *24*(6), 1763–1783, doi:10.1175/2010JCLI3847.1.

Franco-Vizcaíno, E., and J. Sosa-Ramirez (1997), Soil properties and nutrient relations in burned and unburned Mediterranean-climate shrublands of Baja California, Mexico, *Acta Oecol.*, *18*(4), 503–517, doi:10.1016/S1146-609X(97)80037-9.

Grinsted, A., J. C. Moore, and S. Jevrejeva (2004), Application of the cross wavelet transform and wavelet coherence to geophysical time series, *Nonlinear Process. Geophys.*, *11*(5/6), 561–566, doi:10.5194/npg-11-561-2004.

Gu, L., et al. (2005), Objective threshold determination for nighttime eddy flux filtering, *Agric. For. Meteorol.*, *128*, 179–197, doi:10.1016/j.agrformet.2004.11.006.

Jung, M., et al. (2010), Recent decline in the global land evapotranspiration trend due to limited moisture supply, *Nature*, *467*, 951–954, doi:10.1038/nature09396.

Kalthoff, N., M. Fiebig-Wittmaack, C. Meißner, M. Kohler, M. Uriarte, I. Bischoff-Gauß, and E. Gonzales (2006), The energy balance, evapo-transpiration and nocturnal dew deposition of an arid valley in the Andes, *J. Arid Environ.*, *65*, 420–443, doi:10.1016/j.jaridenv.2005.08.013.

Keeley, J. E., and C. J. Fotheringham (2010), History and management of crown-fire ecosystems: A summary and response, *Conserv. Biol.*, *15*(6), 1561–1567.

Kurc, S. A., and E. E. Small (2004), Dynamics of evapotranspiration in semiarid grassland and shrubland ecosystems during the summer monsoon season, central New Mexico, *Water Resour. Res.*, *40*, 1–15, doi:10.1029/2004WR003068.

Lauenroth, W. K., and J. B. Bradford (2009), Ecohydrology of dry regions of the United States: Precipitation pulses and intraseasonal drought, *Ecohydrology*, *2*(2), 173–181, doi:10.1002/eco.53.

Leon, E., R. Vargas, S. Bullock, E. Lopez, A. R. Panosso, and N. La Scala (2014), Hot spots, hot moments, and spatio-temporal controls on soil CO_2 efflux in a water-limited ecosystem, *Soil Biol. Biochem.*, *77*, 12–21, doi:10.1016/j.soilbio.2014.05.029.

Loik, M. E., D. D. Breshears, W. K. Lauenroth, and J. Belnap (2004), A multi-scale perspective of water pulses in dryland ecosystems: Climatology and ecohydrology of the western USA, *Oecologia*, *141*(2), 269–81, doi:10.1007/s00442-004-1570-y.

Longobardi, A., and E. Khaertdinova (2015), Relating soil moisture and air temperature to evapotranspiration fluxes during inter-storm periods at a Mediterranean experimental site, *J. Arid Land*, *7*, 27–36.

Loveland, T. R., B. C. Reed, J. F. Brown, D. O. Ohlen, Z. Zhu, L. Yang, and J. W. Merchant (2000), Development of a global land cover characteristics database and IGBP DISCover from 1 km AVHRR data, *Int. J. Remote Sens.*, *21*, 1303–1330, doi:10.1080/014311600210191.

Maestre, F. T., et al. (2012), Plant species richness and ecosystems multifunctionality in global drylands, *Science*, *335*, 2014–2017.

Méndez-Barroso, L. A., E. R. Vivoni, C. J. Watts, and J. C. Rodríguez (2009), Seasonal and interannual relations between precipitation, surface soil moisture and vegetation dynamics in the North American monsoon region, *J. Hydrol.*, *377*(1–2), 59–70, doi:10.1016/j.jhydrol.2009.08.009.

Méndez-Barroso, L. A., E. R. Vivoni, A. Robles-Morua, G. Mascaro, E. A. Yépez, J. C. Rodríguez, C. J. Watts, J. Garatuza-Payán, and J. A. Saíz-Hernández (2014), A modeling approach reveals differences in evapotranspiration and its partitioning in two semiarid ecosystems in Northwest Mexico, *Water Resour. Res.*, *50*(4), 3229–3252, doi:10.1002/2013WR014838.

Murray, F. W. (1967), On the computation of saturation vapor pressure, *J. Appl. Meteorol.*, *6*, 203–204, doi:10.1175/152050(1967)006<0203:OTCOSV>2.0.CO;2.

Nezlin, N. P., and E. D. Stein (2005), Spatial and temporal patterns of remotely-sensed and field-measured rainfall in southern California, *Remote Sens. Environ.*, *96*, 228–245, doi:10.1016/j.rse.2005.02.005.

Noy-Meir, I. (1973), Desert ecosystems: Environment and producers, *Annu. Rev. Ecol. Syst.*, *4*, 25–51.

Olivier, J. (2004), Fog harvesting: An alternative source of water supply on the West Coast of South Africa, *GeoJournal*, *61*, 203–214, doi:10.1007/s10708-004-2889-y.

Olson, D. M., et al. (2001), Terrestrial ecoregions of the world: A new map of life on Earth, *BioScience*, *51*(11), 933, doi:10.1641/0006-3568(2001)051[0933:TEOTWA]2.0.CO;2.

Perez-Ruiz, E. R., J. Garatuza-Payan, C. J. Watts, J. C. Rodriguez, E. A. Yepez, and R. L. Scott (2010), Carbon dioxide and water vapour exchange in a tropical dry forest as influenced by the North American Monsoon System (NAMS), *J. Arid Environ.*, *74*, 556–563, doi:10.1016/j.jaridenv.2009.09.029.

Porporato, A., P. D'Odorico, F. Laio, L. Ridolfi, and I. Rodriguez-Iturbe (2002), Ecohydrology of water-controlled ecosystems, *Adv. Water Resour.*, *25*(8–12), 1335–1348, doi:10.1016/S0309-1708(02)00058-1.

Potts, D. L., T. E. Huxman, J. M. Cable, D. D. Ignace, J. A. Eilts, M. J. Mason, J. F. Weltzin, and D. G. Williams (2003), Antecedent moisture and seasonal precipitation influence the response of canopy-scale carbon and water exchange to rainfall pulses in a semi-arid grassland, *New Phytol.*, *2*, 849–860.

Poulter, B., et al. (2014), Contribution of semi-arid ecosystems to interannual variability of the global carbon cycle, *Nature*, *509*(7502), 600–603, doi:10.1038/nature13376.

Rana, G., and N. Katerji (2000), Measurement and estimation of actual evapotranspiration in the field under Mediterranean climate: A review, *Eur. J. Agron.*, *13*, 125–153, doi:10.1016/S1161-0301(00)00070-8.

Reichstein, M., et al. (2005), On the separation of net ecosystem exchange into assimilation and ecosystem respiration: Review and improved algorithm, *Global Change Biol.*, *11*, 1424–1439, doi:10.1111/j.1365-2486.2005.001002.x.

Reimer, J. J., R. Vargas, D. Rivas, G. Gaxiola-Castro, J. M. Hernandez-Ayon, and R. Lara-Lara (2015), Sea surface temperature influence on terrestrial gross primary production along the Southern California current, *PLoS One*, *10*(4), e0125177, doi:10.1371/journal.pone.0125177.

Rotenberg, E., and D. Yakir (2010), Contribution of semi-arid forests to the climate system, *Science*, *327*, 451–454, doi:10.1126/science.1179998.

Ryu, Y., D. D. Baldocchi, S. Ma, and T. Hehn (2008), Interannual variability of evapotranspiration and energy exchange over an annual grassland in California, *J. Geophys. Res.*, *113*, D09104, doi:10.1029/2007JD009263.

Sala, O. E., and W. K. Lauenroth (2014), International association for ecology small rainfall events: An ecological role in semiarid regions, *Oecologia*, *53*(3), 301–304.

Schlesinger, W. H., J. F. Reynolds, G. L. Cunningham, L. F. Huenneke, W. M. Jarrell, R. A. Virginia, and W. G. Whitford (1990), Biological feedbacks in global desertification, *Science*, *247*, 1043–1048, doi:10.1126/science.247.4946.1043.

Schwinning, S., and O. E. Sala (2004), Hierarchy of responses to resource pulses in arid and semi-arid ecosystems, *Oecologia*, *141*, 211–220, doi:10.1007/s00442-004-1520-8.

Scott, R. L., P. Serrano-Ortiz, F. Domingo, E. P. Hamerlynck, and A. S. Kowalski (2012), Commonalities of carbon dioxide exchange in semiarid regions with monsoon and Mediterranean climates, *J. Arid Environ.*, *84*, 71–79, doi:10.1016/j.jaridenv.2012.03.017.

Serrano-Ortiz, P., A. S. Kowalski, F. Domingo, A. Rey, E. Pegoraro, L. Villagarcía, and L. Alados-Arboledas (2007), Variations in daytime net carbon and water exchange in a montane shrubland ecosystem in southeast Spain, *Photosynthetica*, *45*(1), 30–35, doi:10.1007/s11099-007-0005-5.

Stoy, P. C., et al. (2009), Biosphere-atmosphere exchange of CO_2 in relation to climate: A cross-biome analysis across multiple time scales, *Biogeosciences*, *6*, 4095–4141, doi:10.5194/bgd-6-4095-2009.

Stoy, P. C., et al. (2013), A data-driven analysis of energy balance closure across FLUXNET research sites: The role of landscape scale heterogeneity, *Agric. For. Meteorol.*, *171–172*, 137–152, doi:10.1016/j.agrformet.2012.11.004.

Sun, L., S. L. Liang, W. P. Yuan, and Z. X. Chen (2013), Improving a Penman-Monteith evapotranspiration model by incorporating soil moisture control on soil evaporation in semiarid areas, *Int. J. Digital Earth*, *6*, 134–156.

Tang, Q., E. R. Vivoni, F. Muñoz-Arriola, and D. P. Lettenmaier (2012), Predictability of evapotranspiration patterns using remotely sensed vegetation dynamics during the North American monsoon, *J. Hydrometeorol.*, *13*(1), 103–121, doi:10.1175/JHM-D-11-032.1.

Torrence, C., and G. P. Compo (1998), A practical guide to wavelet analysis, *Bull. Am. Meteorol. Soc.*, *79*(1), 61–78, doi:10.1175/1520-0477(1998)079<0061:APGTWA>2.0.CO;2.

Vargas, R., et al. (2010), Looking deeper into the soil: Biophysical controls and seasonal lags of soil CO_2 production and efflux, *Ecol. Appl.*, *20*, 1569–1582, doi:10.1890/09-0693.1.

Vargas, R., D. D. Baldocchi, M. Bahn, P. J. Hanson, K. P. Hosman, L. Kulmala, J. Pumpanen, and B. Yang (2011), On the multi-temporal correlation between photosynthesis and soil CO_2 efflux: Reconciling lags and observations, *New Phytol.*, *191*(4), 1006–1017, doi:10.1111/j.1469-8137.2011.03771.x.

Vargas, R., H. W. Loescher, T. Arredondo, E. Huber-Sannwald, R. Lara-Lara, and E. A. Yépez (2012a), Opportunities for advancing carbon cycle science in Mexico: Toward a continental scale understanding, *Environ. Sci. Policy*, *21*, 84–93, doi:10.1016/j.envsci.2012.04.003.

Vargas, R., S. L. Collins, M. L. Thomey, J. E. Johnson, R. F. Brown, D. O. Natvig, and M. T. Friggens (2012b), Precipitation variability and fire influence the temporal dynamics of soil CO_2 efflux in an arid grassland, *Global Change Biol.*, *18*(4), 1401–1411, doi:10.1111/j.1365-2486.2011.02628.x.

Vargas, R., et al. (2013a), Drought influences the accuracy of simulated ecosystem fluxes: A model-data meta-analysis for Mediterranean oak woodlands, *Ecosystems*, *16*, 749–764, doi:10.1007/s10021-013-9648-1.

Vargas, R., et al. (2013b), Progress and opportunities for monitoring greenhouse gases fluxes in Mexican ecosystems: The MexFlux network, *Atmosfera*, *26*(3), 325–336.

Vivoni, E. R. (2012), Spatial patterns, processes and predictions in ecohydrology: Integrating technologies to meet the challenge, *Ecohydrology*, *5*(3), 235–241, doi:10.1002/eco.1248.

Vivoni, E. R., H. A. Moreno, G. Mascaro, J. C. Rodriguez, C. J. Watts, J. Garatuza-Payan, and R. L. Scott (2008), Observed relation between evapotranspiration and soil moisture in the North American monsoon region, *Geophys. Res. Lett.*, *35*, L22403, doi:10.1029/2008GL036001.

Vivoni, E. R., C. J. Watts, J. C. Rodríguez, J. Garatuza-Payan, L. A. Méndez-Barroso, and J. A. Saiz-Hernández (2010a), Improved land-atmosphere relations through distributed footprint sampling in a subtropical scrubland during the North American monsoon, *J. Arid Environ.*, *74*, 579–584, doi:10.1016/j.jaridenv.2009.09.031.

Vivoni, E. R., C. J. Watts, and D. J. Gochis (2010b), Land surface ecohydrology of the North American monsoon system, *J. Arid Environ.*, *74*(5), 529–530, doi:10.1016/j.jaridenv.2009.11.004.

Wang, K., and R. E. Dickinson (2012), A review of global terrestrial evapotranspiration: Observation, modelling, climatology, and climatic variability, *Rev. Geophys.*, *50*, RG2005, doi:10.1029/2011RG000373.

Watts, C. J., R. L. Scott, J. Garatuza-Payan, J. C. Rodriguez, J. H. Prueger, W. P. Kustas, and M. Douglas (2007), Changes in vegetation condition and surface fluxes during NAME 2004, *J. Clim.*, *20*(9), 1810–1820, doi:10.1175/JCLI4088.1.

Weiss, J. L., D. S. Gutzler, J. E. Allred Coonrod, and C. N. Dahm (2004), Seasonal and inter-annual relationships between vegetation and climate in central New Mexico, USA, *J. Arid Environ.*, *57*(4), 507–534, doi:10.1016/S0140-1963(03)00113-7.

Westman, W. E. (1983), Xeric Mediterranean-type shrubland associations of Alta and Baja California and the community/continuum debate*, *Vegetatio*, *52*(1), 3–19.

Wetzel, P. J., and J. T. Chang (1987), Concerning the relationship between evapotranspiration and soil moisture, *J. Clim. Appl. Meteorol.*, *26*, 18–27.

Wilson, K., et al. (2002), Energy balance closure at FLUXNET sites, *Agric. For. Meteorol.*, *113*, 223–243, doi:10.1016/S0168-1923(02)00109-0.

Yepez, E. a., R. L. Scott, W. L. Cable, and D. G. Williams (2007), Intraseasonal variation in water and carbon dioxide flux components in a semiarid riparian woodland, *Ecosystems*, *10*(7), 1100–1115, doi:10.1007/s10021-007-9079-y.